Available online at www.sciencedirect.com
SCIENCE DIRECT®
Thermochimica Acta 419 (2004) 223–229
thermochimica acta
www.elsevier.com/locate/tca

Thermal decomposition of $[Mg(NH_3)_6](NO_3)_2$, $[Ni(NH_3)_6](NO_3)_2$ and $[Ni(ND_3)_6](NO_3)_2$

A. Migdał-Mikuli [a,*], E. Mikuli [a], R. Dziembaj [b], D. Majda [c], Ł. Hetmańczyk [a]

[a] *Department of Chemical Physics, Faculty of Chemistry of the Jagiellonian University, ulica Ingardena 3, 30-060 Cracow, Poland*
[b] *Department of Chemical Technology, Faculty of Chemistry of the Jagiellonian University, ulica Ingardena 3, 30-060 Cracow, Poland*
[c] *Regional Laboratory of Physicochemical Analysis and Structural Research, Jagiellonian University, ulica Ingardena 3, 30-060 Cracow, Poland*

Received 21 May 2003; received in revised form 8 January 2004; accepted 30 January 2004

Available online 21 April 2004

Abstract

The thermal decompositions of $[Mg(NH_3)_6](NO_3)_2$, $[Ni(NH_3)_6](NO_3)_2$ and $[Ni(ND_3)_6](NO_3)_2$ were studied by thermal gravimetry analysis (TGA) and simultaneous differential thermal analysis (SDTA) at a constant heating rate. The gaseous products of the decomposition were on-line identified by a quadruple mass spectrometer (QMS).The solid products were identified on the basis of Fourier transform mid infrared spectra (FT-MIR) and X-ray powder diffraction (XRPD) patterns. Deamination of hexaaminemagnesium nitrate(V) to diaminemagnesium nitrate(V) undergoes in *two steps* and *two-third* of the all NH_3 molecules are liberated. Deamination of both hexaaminenickel(II) nitrates(V) (non-deuterated and deuterated) to the diamines undergoes in *three steps*, and at two first steps *one half* of the NH_3 molecules are liberated. The thermal decomposition of $[Ni(NH_3)_2](NO_3)_2$ and $[Ni(ND_3)_2](NO_3)_2$ is also different than that of $[Mg(NH_3)_2](NO_3)_2$. In both cases the decomposition is connected with the redox processes, but in the case of magnesium compound, contrary to the nickel compounds, in the second stage, besides of liberation of nitrogen, nitrogen oxides and H_2O, undergoes the liberation of NH_3 and the formation of $Mg(NO_3)_2$, which in turn decomposes next, in the third stage, to the oxygen, nitrogen oxides and MgO. This third stage is not present in the case of both nickel compounds, and the decomposition of diaminenickel(II) nitrates(V) undergoes directly to the final products (NiO_{1+x}, nitrogen, nitrogen oxides and H_2O) without the formation of $Ni(NO_3)_2$, because of the autocatalytic effect of the formed NiO.

Keywords: Hexaaminemagnesium and hexaaminenickel(II) nitrates(V); Thermal decomposition; TGA; DTA; QMS; FT-MIR; XRPD

1. Introduction

It is a well-known fact that the title compounds exhibit interesting phase polymorphism and large thermal hysteresis of phase II ↔ phase III transition, which is connected with the freezing (→) or set in motion (←) the fast reorientation (i.e. reorientational correlation time amounts to several picoseconds) of a characteristic part of the NH_3 groups (see Ref. [1,2] and the papers quoted there). In phase I and phase II of these compounds all NH_3 groups reorientate fast. On cooling these compounds down, after the phase transition: phase II → phase III, in the case of $[Ni(NH_3)_6](NO_3)_2$ (and of $[Ni(ND_3)_6](NO_3)_2$ too) only *one half* of the so far fast reorientating NH_3 (ND_3) groups stop this fast reorientation, whereas, in the case of $[Mg(NH_3)_6](NO_3)_2$ only *two-third* of the NH_3 groups freeze its fast reorientation. However, while these compounds are heated up, the reorientation of the above mentioned parts of the NH_3 groups, which was "frozen", resumes gradually just before the phase transition: phase III → phase II. After the transition to the phase II all of the NH_3 groups already reorientate fast. The phase III → phase II transition on heating the compounds studied takes place at a much higher temperature (T^h_{C2}) than the phase transition phase II → phase III on cooling them (T^c_{C2}). The difference between these two phase transition temperatures ($T^h_{C2} - T^c_{C2}$) defines the width of the thermal hysteresis loop of the phase II ↔ phase III transition. For $[Ni(NH_3)_6](NO_3)_2$ the width of the thermal hysteresis loop is ca. 90 K, for $[Ni(ND_3)_6](NO_3)_2$ it is ca.106 K, and for $[Mg(NH_3)_6](NO_3)_2$ it is ca. 35 K [1–5].

The aim of this study is to determine whether the above described picture of the molecular reorientational motions of the title compounds has some correlations with the mechanism of their thermal deamination and what are the

* Corresponding author. Tel.: +48-12-633-63-77x2256; fax: +48-12-634-05-15.
E-mail address: migdalmi@chemia.uj.edu.pl (A. Migdał-Mikuli).

0040-6031/$ – see front matter © 2004 Elsevier B.V. All rights reserved.
doi:10.1016/j.tca.2004.01.035

differences in the thermal decomposition of their deamination products.

2. Experimental

The chemical synthesis of the title compounds was described elsewhere [3–5].

A characterization of the decomposition process of the title compounds was performed using a Mettler Toledo TGA/SDTA 851^e apparatus. Samples of masses given in Tables 1–4 were placed in 150 μl corundum crucibles. The thermo gravimetric analysis (TGA) measurements were made in a flow of Argon from 300 up to 1000 K. The TGA measurements were performed at a *constant heating rate* of 10 K min^{-1}. At a constant heating rate besides TG and DTG curves, the simultaneous differential thermal analysis (SDTA) curve and the simultaneous evolved gas analysis (SEGA), with on-line quadruple mass spectrometer (QMS) using a Balzer GSD 300T apparatus, were also registered. The temperature was measured by a Pt–Pt/Rh thermocouple with the accuracy of ±0.5 K.

The X-ray powder diffraction (XRPD) analysis of the solid decomposition products was made with a Philips X'Pert PRO apparatus using filtrated Cu Kα_1 radiation.

The spectroscopic identification of the deamination products was performed using a Bruker EQUINOX-55 spectrometer. The Fourier transform mid infrared (FT-MIR) measurements were made in the frequency range of 400–4000 cm^{-1} with the resolution of 2 cm^{-1}.

3. Results and discussion

3.1. Decomposition of $[Mg(NH_3)_6](NO_3)_2$

Fig. 1 shows TG, DTG, QMS and DTA curves recorded for $[Mg(NH_3)_6](NO_3)_2$ at a constant heating rate of 10 K min^{-1} in the temperature range of 300–1000 K. During the TG experiment, the QMS spectrum of masses were followed from $m/e = 1$ to 100, however, for reasons of graphic readability, only the masses of $m/e = 17$, 18, 28, 30, 32 and 44—representing NH_3, H_2O, N_2, NO, O_2 and N_2O are shown. The QMS spectrum of mass $m/e = 17$ represents also the OH fragment of H_2O fragmentation, which was taken into account in the determination of NH_3 concentration. The temperatures, percentage mass losses and the products of the decomposition at particular stages are presented in Table 1.

The TG, DTG and QMS curves show that the decomposition of the sample proceeds in *three* main stages. It can be observed that the first stage involves the step-wise freeing of four NH_3 molecules. The composition of the $[Mg(NH_3)_2](NO_3)_2$, the final product of the deamination processes, was confirmed by the chemical analysis and the FT-MIR spectrum. The second stage is connected with the

Table 1
Parameters of $[Mg(NH_3)_6](NO_3)_2$ thermal analysis

Sample mass (mg)	Stage number	Temperature range (K)	Mass loss at the stage (%)	Mass after decomposition (%)	Calculated values (%)	Products of the decomposition
24.2809	Ia	300–391	11.6		13.6	$2NH_3$
	Ib	392–496	15.4		13.6	$2NH_3$
	IIa, IIb, IIc	497–607	19.8		56.7	$2H_2O + 1\frac{1}{3}NO + \frac{2}{3}N_2O + \frac{2}{3}H_3 + \frac{1}{3}N_2 + \frac{1}{2}O_2$
	III	608–850	35.1			
				18.1	16.1	MgO

Table 2
Parameters of $[Mg(H_2O)_6](NO_3)_2$ thermal analysis

Sample mass (mg)	Stage number	Temperature range (K)	Mass loss at the stage (%)	Mass after decomposition (%)	Calculated values (%)	Products of the decomposition
163.924	Ia	300–550	35.02		35.13	$5H_2O$
	Ib	551–620	6.93		7.03	$1H_2O$
	II	621–770	41.85		42.13	$2NO + 1\frac{1}{2}O_2$
				16.20	15.71	MgO

Table 3
Parameters of $[Ni(NH_3)_6](NO_3)_2$ thermal analysis

Sample mass (mg)	Stage number	Temperature range (K)	Mass loss at the stage (%)	Mass after decomposition (%)	Calculated values (%)	Products of the decomposition
30.4147	Ia	300–475	12.0		11.9	$2NH_3$
	Ib	476–507	6.3		6.0	$1NH_3$
	Ic	508–545	6.0		6.0	$1NH_3$
	II	546–850	49.5		49.9	$3H_2O + NO + N_2O + \frac{1}{2}N_2$
				26.2	26.2	NiO

Table 4
Parameters of $[Ni(ND_3)_6](NO_3)_2$ thermal analysis

Sample mass (mg)	Stage number	Temperature range (K)	Mass loss at the stage (%)	Mass after decomposition (%)	Calculated values (%)	Products of the decomposition
22.9349	Ia	300–462	12.9		13.2	$2ND_3$
	Ib	463–489			6.6	$1ND_3$
	Ic	490–570	13.5		6.6	$1ND_3$
	II	570–850	48.8		48.9	$3D_2O + NO + N_2O + \frac{1}{2}N_2$
				24.8	24.7	NiO

simultaneous liberation of ammonia, water and magnesium oxide and the third stage with decomposition of resulting $Mg(NO_3)_2$ to nitrogen oxides species, oxygen and solid MgO. 18.1% of the initial mass of the sample remained after the second stage of the decomposition and this figure corresponds to the amount of magnesium oxide (see Table 1).

The profile of the SDTA curve of $[Mg(NH_3)_6](NO_3)_2$ shows three endothermic peaks and one exothermic peak. The first two small endothermic peaks can be explained by the *two steps of the deamination* resulting in the formation of the tetra- and diamine, according to the following reactions:

$$\text{Ia}: \quad [Mg(NH_3)_6](NO_3)_2 \rightarrow [Mg(NH_3)_4](NO_3)_2 + 2NH_3,$$
$$\text{Ib}: \quad [Mg(NH_3)_4](NO_3)_2 \rightarrow [Mg(NH_3)_2](NO_3)_2 + 2NH_3. \qquad (1)$$

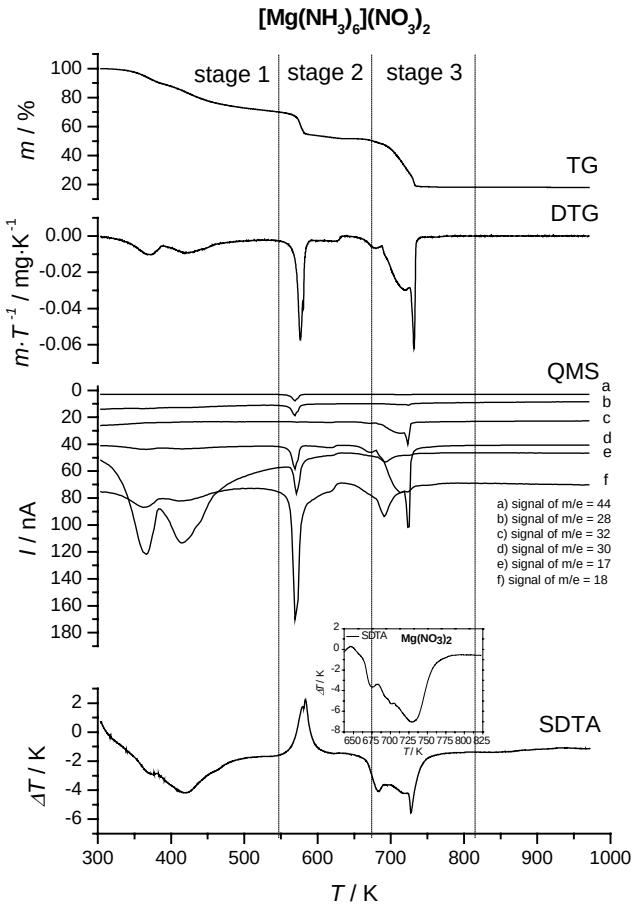

Fig. 1. TG, DTG, QMS and SDTA curves for $[Mg(NH_3)_6](NO_3)_2$ in the range of 300–1000 K, heated at a constant heating rate of 10 K min^{-1}.

The composition of the $[Mg(NH_3)_2](NO_3)_2$ was confirmed by the chemical analysis and the FT-MIR spectrum.

The exothermic peak can be explained on the basis of redox processes during the decomposition of the diamine complex, according to the reactions:

$$\text{IIa}: \quad [Mg(NH_3)_2](NO_3)_2 \rightarrow MgO + N_2 + 2NO + 3H_2O,$$
$$\text{IIb}: \quad [Mg(NH_3)_2](NO_3)_2 \rightarrow MgO + 2N_2O + 3H_2O,$$
$$\text{IIc}: \quad [Mg(NH_3)_2](NO_3)_2 \rightarrow Mg(NO_3)_2 + 2NH_3. \qquad (2)$$

The first two reactions (IIa and IIb) are not going completely, because $Mg(NO_3)_2$ in the last stage decomposes to oxygen, nitrogen oxides and solid MgO, according to the following reactions:

$$\text{III}: \quad Mg(NO_3)_2 \rightarrow MgO + (N_2O_5) \rightarrow MgO + \tfrac{1}{2}O_2 + N_2O_4$$
$$\rightarrow MgO + \tfrac{1}{2}O_2 + 2NO_2 \leftrightarrow MgO + 2NO + 1\tfrac{1}{2}O_2. \qquad (3)$$

The third broad and split endothermic peak in SDTA curve, which is registered just after the exothermic peak, is connected with presented above decomposition of the $Mg(NO_3)_2$.

In order to better recognition of the thermal decomposition process of $Mg(NO_3)_2$ in a flow of Argon, we performed the thermal analysis of polycrystalline $[Mg(H_2O)_6](NO_3)_2$. TG, DTG and SDTA curves are presented in Fig. 2. Thermal decomposition process has two main parts: one connected with the dehydration and the second with decomposition of anhydrous magnesium nitrate to magnesium oxide, nitrogen oxide and oxygen. The dehydration undergo in two steps: at first step five H_2O molecules per formula unit and at the second step the last one H_2O are freeing. Two thermal dehydration processes of $[Mg(H_2O)_6](NO_3)_2$ presented by Odochian [6], one in a flow of ambient atmosphere and the second in a flow of nitrogen at 30 ml min^{-1}, are very similar to that presented by us in a flow of Argon. The fragment of the SDTA curve, which was connected with the decomposition of anhydrous $Mg(NO_3)_2$ we added as an insertion in Fig. 1 in order to compare the obtained results. The decomposition of $Mg(NO_3)_2$ undergo in a way presented in Eq. (3). The temperatures, percentage mass losses and the products of the decomposition of $[Mg(H_2O)_6](NO_3)_2$ at particular stages are presented in Table 2.

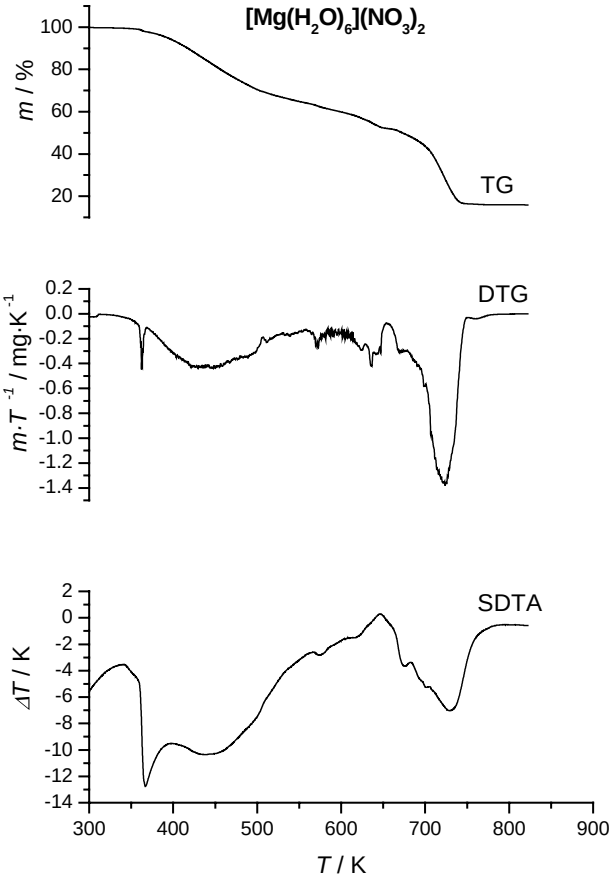

Fig. 2. TG, DTG and SDTA curves for $[Mg(H_2O)_6](NO_3)_2$.

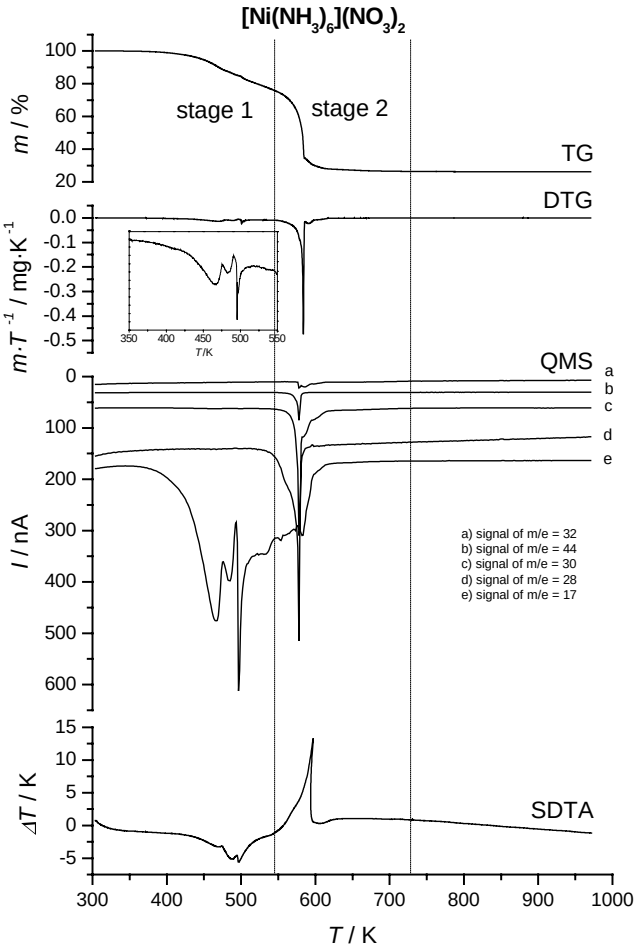

Fig. 3. TG, DTG, QMS and SDTA curves for $[Ni(NH_3)_6](NO_3)_2$ in the range of 300–1000 K, heated at a constant heating rate of 10 K min^{-1}.

3.2. Decomposition of $[Ni(NH_3)_6](NO_3)_2$ and $[Ni(ND_3)_6](NO_3)_2$

Fig. 3 shows TG, DTG, QMS and SDTA curves recorded for $[Ni(NH_3)_6](NO_3)_2$ at a constant heating rate of 10 K min^{-1} in the temperature range of 300–1000 K. During the TG experiment, the QMS spectra of masses were followed from $m/e = 1$ to 100, however, for reasons of graphic readability, only the masses of $m/e = 17$, 18, 28, 30, 32 and 44—representing NH_3, H_2O, N_2, NO, O_2 and N_2O are shown. The QMS spectrum of mass $m/e = 17$ represents also the OH fragment of H_2O fragmentation. The temperatures, percentage mass losses and the products of the decomposition at particular stages are presented in Table 3.

The TG, DTG and QMS curves show that the decomposition of the sample proceeds in *two* main stages. It can be observed that the first stage involve mainly the step-wise freeing of four NH_3 molecules (partial deamination), whereas the second stage—with the decomposition of $[Ni(NH_3)_2](NO_3)_2$ to nitrogen, nitrogen oxides, water and solid NiO.

The profile of the SDTA curve of $[Ni(NH_3)_6](NO_3)_2$ shows three small endothermic peaks and one broad, big exothermic peak. The endothermic peaks can be explained by the *three steps of the deamination* resulting in the formation of the tetra-, tri- and diamine, in succession, according to the following reactions:

$$\begin{aligned}
&\text{Ia}: \quad [Ni(NH_3)_6](NO_3)_2 \rightarrow [Ni(NH_3)_4](NO_3)_2 + 2NH_3,\\
&\text{Ib}: \quad [Ni(NH_3)_4](NO_3)_2 \rightarrow [Ni(NH_3)_3](NO_3)_2 + NH_3,\\
&\text{Ic}: \quad [Ni(NH_3)_3](NO_3)_2 \rightarrow [Ni(NH_3)_2](NO_3)_2 + NH_3.
\end{aligned} \tag{4}$$

The composition of the $[Ni(NH_3)_2](NO_3)_2$, the final product of the deamination process Ic (4), was confirmed by the chemical analysis and the FT-MIR spectrum. Fig. 4 shows the comparison of the FT-MIR spectra of the hexaamine- and diamine-nickel(II) nitrates(V), the substrate and the final product of the deamination process Ic (4), respectively.

The third endothermic peak is immediately followed by a broad and big exothermic peak, contrary to the expected enthalpy changes accompanying the decomposition of a stable $[Ni(NH_3)_2](NO_3)_2$ complex. The exothermic peak for $[Ni(NH_3)_2](NO_3)_2$ can be explained by reduction and oxidation (redox) processes taking place between the reductants (NH_3 ligands) and the oxidants (NO_3^-). The beginning of the exothermic effect (at 550 K) is correlated with beginning

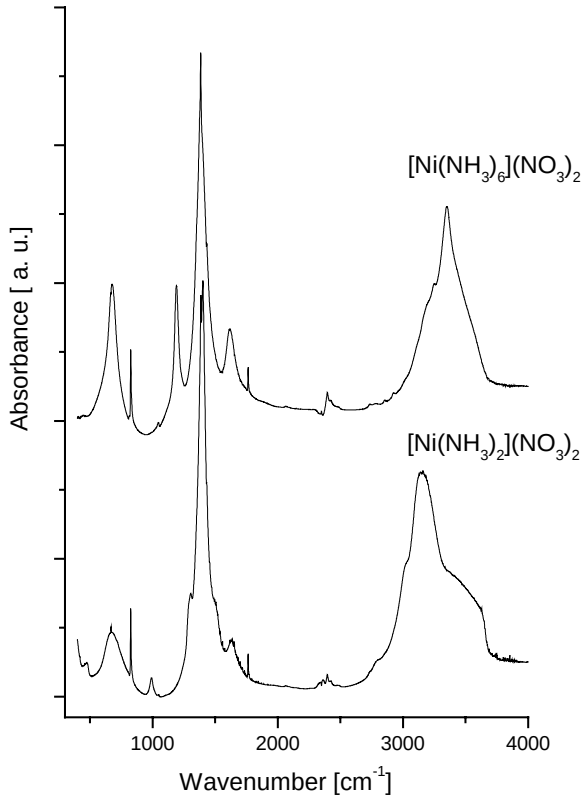

Fig. 4. Comparison of the FT-MIR spectra of $[Ni(NH_3)_6](NO_3)_2$ (substrate) and $[Ni(NH_3)_2](NO_3)_2$ (final product of the deamination processes Ia, Ib and Ic).

of N_2 molecules evolution observed in the simultaneous evolved gas analysis (SEGA) with on-line QMS. The acceleration of exothermic effect is bounded with acceleration of N_2 production and additional evolution of N_2O. Therefore, the redox process is composed of two overall reactions:

$$\text{IIa}: \quad [Ni(NH_3)_2](NO_3)_2 \rightarrow NiO + N_2 + 2NO + 3H_2O,$$

$$\text{IIb}: \quad [Ni(NH_3)_2](NO_3)_2 \rightarrow NiO + 2N_2O + 3H_2O. \qquad (5)$$

26.2% of the initial mass of the sample remained after the second stage of the decomposition and this figure corresponds to the amount of nickel oxide (see Table 3). The XRPD analysis of the solid decomposition product confirmed that it was NiO, which has the cubic structure (Fm3m, $a = 4.1761$ Å), as identified using ICDD No. 47-1049 data.

The role of transition metal cation in processes IIa and IIb should not be ignored. Thermal decomposition of nickel nitrate results in formation of non-stoichiometric NiO_{1-x}. Małecki et al. [7,8] showed that the concentration of Ni^{3+} in the decomposition product achieve 1 at.% of Ni^{3+}. The non-stoichiometric nickel oxide can catalyse many redox reactions. Perhaps, the delay in appearance of NO in the gaseous products arose from a secondary reaction:

$$NiO + xNO = NiO_{1+x} + xN_2. \qquad (6)$$

The system of Ni^{3+}/Ni^{2+} with anionic vacancies in the oxide lattice can work as electron and oxygen transmitters between reductive NH_3 molecules and oxidative nitrate ions or nitrogen oxides. The rate acceleration in the case of the second stage of the thermal decomposition, namely during $[Ni(NH_3)_2](NO_3)_2$ final decomposition, may be caused by an autocatalytic effect of the decomposition product NiO_{1+x}. Ettarh and Galway [9,10] showed that transition metal oxides, among them NiO, catalyse thermal decomposition of $Co(NO_3)_2$. A very similar complex compound, $[Co(NH_3)_6](NO_3)_2$, decomposes according to Wendlandt and Smith [11] in two steps. During the first step $[Co(NH_3)_4](NO_3)_2$ is formed (at about 410 K). Above 480 K the tetraaminecobalt(II) nitrate(V) is decomposed very rapidly with formation of H_2O, N_2 and Co_3O_4, besides NH_3 [11].

Fig. 5 shows TG, DTG and DTA curves recorded for $[Ni(ND_3)_6](NO_3)_2$ at a constant heating rate of 10 K min^{-1} in the temperature range 300–1000 K. The temperatures, percentage mass losses and the products of the decomposition at particular stages are presented in Table 4. The thermogravimetric measurements for both isotope specimens show that the decomposition of the deuterated compound proceeds, very similar like in the case of nondeuterated one, in *two* main stages. First stage involves mainly the step-wise

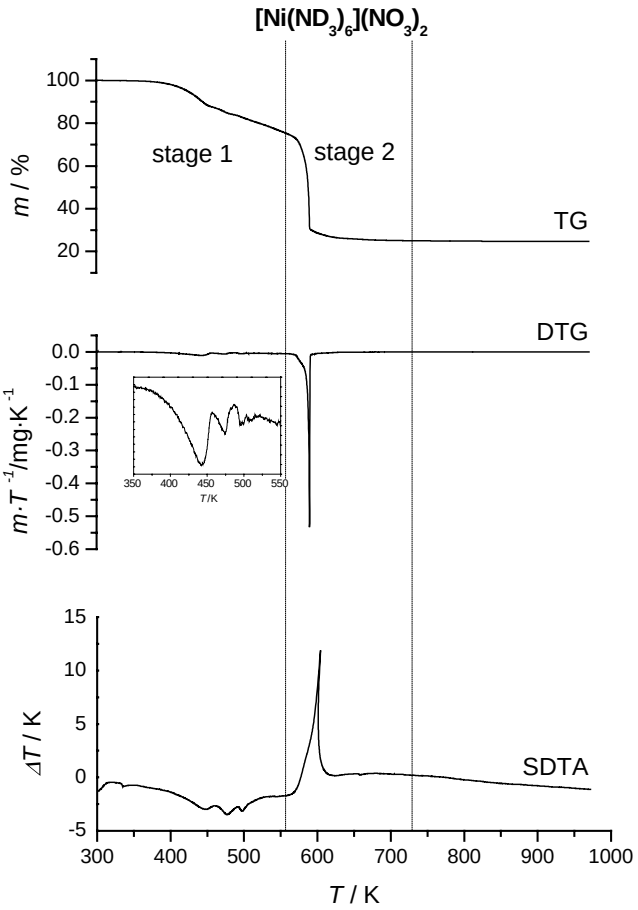

Fig. 5. TG, DTG and SDTA curves for $[Ni(ND_3)_6](NO_3)_2$ in the range of 300–1000 K, heated at a constant heating rate of 10 K min^{-1}.

freeing of four ND_3 molecules, whereas the second stage mainly the decomposition of $[Ni(ND_3)_2](NO_3)_2$ to nitrogen, nitrogen oxides, heavy water and NiO. The composition of the $[Ni(ND_3)_2](NO_3)_2$, the final product of the deamination processes, was confirmed by the chemical analysis and the FT-MIR spectrum.

24.8% of the initial mass of the sample remained after the second stage of the decomposition and this figure corresponds to the amount of nickel oxide (see Table 4). The XRPD analysis of the solid decomposition product confirmed that it was NiO, which has the cubic structure (Fm3m, $a = 4.176$ Å), as identified using ICDD No. 47-1049 data. Because of a great similarity of the mechanism of the thermal decompositions of both isotope specimens we did not recorded the QMS spectrum during the TG experiment for $[Ni(ND_3)_6](NO_3)_2$. Moreover, it would demand exchange of Ar into Ne as the current and eluent gas.

The profile of the SDTA curve of $[Ni(ND_3)_6](NO_3)_2$ shows three endothermic peaks and one single exothermic peak. The endothermic peaks can be explained by the three stages of the deamination resulting in the formation of the tetra-, tri- and diamine, according to reactions that are very similar to reactions (4). The third endothermic peak is immediately followed by a sharp exothermic peak The exothermic peak can be explained on the basis of redox processes during the decomposition of the diamine complex, according to the reactions very similar to reactions (5).

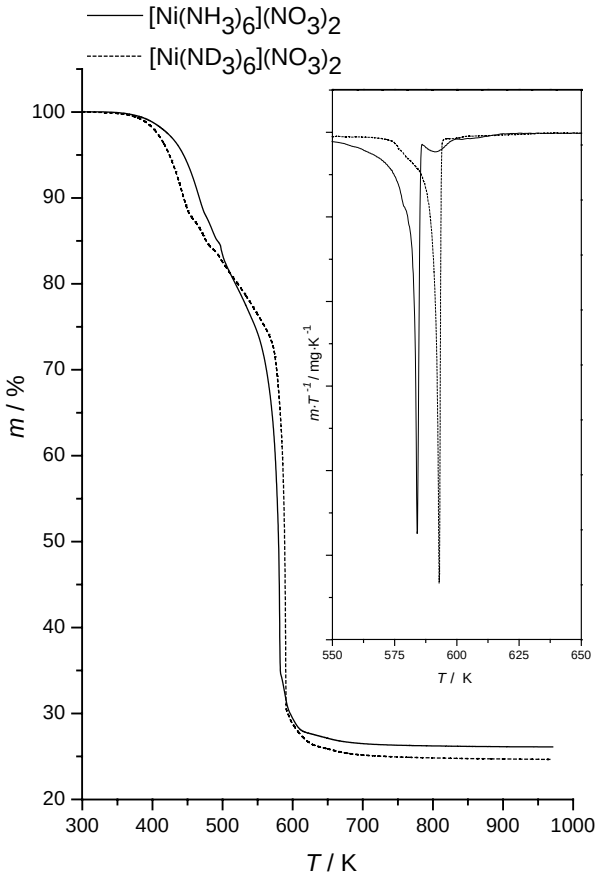

Fig. 6. Comparison of TG and DTG curves for $[Ni(NH_3)_6](NO_3)_2$ and $[Ni(ND_3)_6](NO_3)_2$.

Comparing the thermal decomposition processes of $[Ni(NH_3)_6](NO_3)_2$ and $[Ni(ND_3)_6](NO_3)_2$, registered at a constant heating rate in a flow of Argon, we noticed that they proceed in an almost identical way. The main difference is in a kinetic isotope effect. Fig. 6 shows comparison of the DTG curves for the deuterated and non-deuterated compound. It can be seen that the particular NH_3 ligands are liberated in a slightly lower temperature than the ND_3 ones.

4. Conclusions

1. The thermal decomposition processes of $[Ni(NH_3)_6](NO_3)_2$ and $[Ni(ND_3)_6](NO_3)_2$ to respective diamines are very similar. Whereas, the thermal decomposition of $[Mg(NH_3)_6](NO_3)_2$ to diaminemagnesium nitrate(V) is slightly different. In the case of hexaaminenickel(II) nitrate(V) compounds the liberation of NH_3 (ND_3) undergoing in the *three steps* and only *one half* of the NH_3 (ND_3) molecules ($2/6 + 1/6 = 1/2$) are initially liberated, and in the case of hexaaminemagnesium nitrate(V) compound the liberation undergoes in *two steps* and *two-third* of the NH_3 molecules ($2/6 + 2/6 = 2/3$) are liberated. A possible reason of that difference is that in the case of nickel compounds one half, and in the case of magnesium compound two thirds, of all NH_3 molecules are bonded weaker to the central metal atom than the rest molecules, probably because of they take a part in a stronger hydrogen bonds with oxygen atoms from NO_3^- anions. Thus, the reorientational motions of this part of NH_3 molecules may be frozen earlier than that of the rest. If this is true, there is a great similarity between the different manner of the liberation of the NH_3 ligands and the different character of the orientational order-disorder process of these ligands in hexaaminenickel(II) nitrate(V) and in hexaaminemagnesium nitrate(V).
2. The thermal decomposition of $[Mg(NH_3)_2](NO_3)_2$ is also different than that of $[Ni(NH_3)_2](NO_3)_2$ and $[Ni(ND_3)_2](NO_3)_2$. In both cases the decomposition is connected with the redox processes, but in the case of magnesium compound, contrary to the nickel compounds, in the second stage, besides of liberation of nitrogen, nitrogen oxides and H_2O, undergoes the liberation of NH_3 and the formation of $Mg(NO_3)_2$, which in turn decomposes next, in the third stage, to the oxygen, nitrogen oxides and MgO. This third stage is not present in the case of both nickel compounds, and the decomposition of diaminenickel(II) nitrates(V) undergoes directly to the final products (NiO_{1+x}, nitrogen, nitrogen oxides and H_2O) without the formation of $Ni(NO_3)_2$, because of the autocatalytic effect of the formed NiO.

Acknowledgements

Appreciations are due to Dr. M. Buæko, who made the X-ray measurements and to I. Szpyt M.Sc., who registered for us the FT-MIR spectra.

References

[1] A. Migdał-Mikuli, E. Mikuli, Acta Phys. Polon. A 88 (1995) 527.
[2] J.M. Janik, J.A. Janik, A. Migdał-Mikuli, E. Mikuli, K. Otnes, Physica B 168 (1991) 45.
[3] A. Migdał-Mikuli, E. Mikuli, M. Rachwalska, T. Stanek, J.M. Janik, J.A. Janik, Physica B 104 (1981) 331.
[4] A.F. Andresen, H. Fjellvåg, J.A. Janik, J. Mayer, J. Ściesiński, J.M. Janik, A. Migdał-Mikuli, E. Mikuli, M. Rachwalska, T. Stanek, Physica B 138 (1986) 295.
[5] J.A. Janik, J.M. Janik, A. Migdał-Mikuli, E. Mikuli, M. Rachwalska, T. Stanek, K. Otnes, B.O. Fimland, I. Svare, Physica B 122 (1983) 315.
[6] L. Odochian, J. Thermal Anal. 45 (1995) 1437.
[7] A. Małecki, R. Gajewski, S. Łabuś, B. Prochowska-Klisch, K. Wojciechowski, J. Thermal Anal. 39 (1993) 545.
[8] A. Małecki, R. Gajewski, S. Łabuś, B. Prochowska-Klisch, K.T. Wojciechowski, J. Thermal Anal. 60 (2000) 17.
[9] C. Ettark, A.K. Galwey, Thermochim. Acta 261 (1995) 125.
[10] C. Ettark, A.K. Galwey, Thermochim. Acta 288 (1996) 203.
[11] W.W. Wendlandt, J.P. Smith, J. Inorg. Nucl. Chem. 25 (1963) 985.